Temperature dependent dielectric spectroscopy of muscle tissue phantom

Ondrej Fiser[1] (iD), Sebastian Ley[2], Marko Helbig[2], Jürgen Sachs[3], Michaela Kantova[4] and Jan Vrba[4]

[1]Department of Biomedical Technology, Faculty of Biomedical Engineering, CTU in Prague, Prague, Czech Republic; [2]Faculty of Computer Science and Automation, Institute of Biomedical Engineering and Informatics, TU Ilmenau, Ilmenau, Germany; [3]Ilmsens GmbH, Ilmenau, Germany and [4]Department of Electromagnetic Field, Faculty of Electrical Engineering, CTU in Prague, Prague, Czech Republic

Abstract

The temperature dependence of the dielectric parameters of tissues and tissue-mimicking phantoms is very important for non-invasive temperature measurement in medical applications using microwaves. We performed measurements of this dependence in the temperature range of 25–50°C using distilled water as a reference liquid commonly used in dielectric property studies. The results were compared with the literature model in the frequency range of 150–3000 MHz. Using this method, the temperature dependence of dielectric parameters of a new muscle tissue-mimicking phantom based on agar, polyethylene powder, and polysaccharide material TX-151 was measured in the temperature range of 25–50°C. The temperature dependence of the dielectric properties of this new muscle phantom was fitted to that of the two-pole Cole–Cole model and the deviation of the results between measured and modeled data was quantified.

Introduction

Cancer treatment is one of the most challenging fields in medicine. Cancer is the second cause of death in the world. Hyperthermia is an adjuvant oncological treatment, where the main goal is to heat up the tumorous tissue by 4–8°C [1]. It is evident that the combination of common treatments (e.g. radiotherapy or chemotherapy) with hyperthermia brings the benefits for patients (5-year survival rate) [2].

In order to meet the safety requirements of the hyperthermia treatment, continuous temperature monitoring is needed. The most used method is applying optical catheters which are injected into the heated area. That is very uncomfortable for the patient. To overcome this issue, non-invasive methods are being developed. Among them, we consider differential temperature monitoring using UWB radar. In our previous feasibility studies, we demonstrated the possibility to detect the reflected signal changes (differences) from the heated region in human tissue-mimicking phantoms [3,4]. This approach is based on the reflected differential signal intensity from the heated region. A differential signal is caused by the temperature dependence of the dielectric parameters, which is creating contrast in the local heated area. The amount of change in dielectric parameters of different tissues can be assigned to the water content in the tissue. Due to the higher water content in human tissues, the relative permittivity and effective conductivity are decreasing on frequencies above 2500 MHz during heating.

Proposing the specific temperature measurement system requires precise numerical simulations. That needs valid input data about the changes in the dielectric parameters of different temperature changes. A lot of extensive studies of dielectric parameters can be found in the literature, but most of them were measured at constant room temperature. As far as we know there is a study made by the team of Lazebnik, where the temperature dependence of complex permittivity of the pork livers is measured and modeled [5]. In our previous study, the approach of the dielectric parameters using UWB M-sequence radar measurement was presented [6,7].

The main purpose of this paper is to verify our approach of the measurement of the temperature-dependent dielectric parameters using new muscle phantom intended for testing of hyperthermia systems combined with UWB radar for the determination of the differential temperature profile. From the measurement of the temperature dependency of the dielectric parameters of the muscle tissue phantom, the temperature-dependent Cole–Cole parameters were estimated.

Measurement of temperature-dependent dielectric parameters

For the temperature-dependent dielectric spectroscopy, an open-ended coaxial probe was used. The principle of the method is based on the 1-port reflection (S_{11}) measurement.

CAMBRIDGE
UNIVERSITY PRESS

Measurement setup

The measurement setup was proposed to reach high accuracy and suppress any uncertainties. We used dielectric probe SPEAG DAK-12, which is able to perform measurements in the frequency range of 4–3000 MHz [8]. The dielectric probe was fed vial coaxial cable from the handheld network-vector analyzer Keysight N9913A FieldFox being connected to PC with software for the calculation of dielectric parameters developed by SPEAG (Switzerland). The whole medium under test (MUT) and the probe were immersed in a container filled by distilled water tempered to the exact temperature of the measurement. To avoid cable and probe movements, the container and MUT were placed on a lifting table.

The measurement setup for the temperature-dependent spectroscopy of dielectric parameters is shown in Fig. 1(a). Figure 1(b) depicts the water container with the dielectric probe and two tissue mimicking-phantoms. In the control sample two temperature probes were inserted.

Temperature-dependent calibration

In our preliminary measurements, the probe calibration was realized by a three-term calibration (open, short and matching liquid). As a reference liquid, the 0.1 M saline solution was used. The calibration was performed only at laboratory temperature (20°C).

According to our initial results from [6], the difference between the measured temperature dependence of distilled water and the Ellison model [9] can be reduced by performing the temperature calibration. To do this, the probe, short, and reference liquid were preheated to the temperature during which the calibration was performed. The temperature calibration was done at seven temperatures in the range of 20–50°C at the 5°C intervals.

Statistical evaluation of measurement

The measurement was performed 10 times at each considered temperature. From that data the mean value together with the standard deviation (uncertainty type A – u_A) was calculated. From the data sheet [8] provided by the manufacturer of the dielectric probe the probe uncertainty at each frequency band was taken (uncertainty type B – u_B). Both types of error are considered as statistically independent from each other. The measured results in this paper are presented with the combined standard uncertainty (uncertainty type C – u_C) calculated according to the following equation (1), which is presented in the graphs.

$$u_C = \sqrt{u_A^2 + u_B^2} \qquad (1)$$

Measurement procedure and accuracy

Figure 1 illustrates a measurement setup for the temperature-dependent spectroscopy of the muscle phantoms. The temperature-dependent calibration was performed before the start of the measurement. Two identical tissue-mimicking phantoms were inserted into the heated water. In the control sample two temperature probes were inserted (one in the center, second to the edge of the phantom). The probe was immersed in water

and attached to the MUT. The water in the container was heated to the temperature of measurement and the temperature of the controlling sample was observed. When the difference between temperature (T_1 and T_2) was less than 0.2°C, the phantom was taken as uniformly heated. The calibration for this temperature was loaded and the measurement was performed.

For the accuracy evaluation, the dielectric parameters of the distilled water were measured in the temperature range of 25–45°C. The complex relative permittivity is defined as follows:

$$\varepsilon^*(f, T) = \varepsilon'(f, T) - i\varepsilon''(f, T) \qquad (2)$$

where ε^* is the complex permittivity, ε' is the relative permittivity, ε'' represents the dielectric loss, f is the frequency, and T is the temperature. The dielectric loss can be transformed into the effective conductivity σ according to the following formula:

$$\sigma(f, T) = 2\pi f \varepsilon_0 \varepsilon''(f, T) \qquad (3)$$

where ε_0 is the permittivity of free space.

In Fig. 2 the results of the measurement (relative permittivity $\varepsilon'(f, T)$ and effective conductivity $\sigma(f, T)$) are presented (solid lines). This measurement was performed after the temperature-dependent calibration. The dashed lines are presenting the Ellison model [9].

The relative permittivity and effective conductivity are decreasing with the increasing temperature. This corresponds to the Ellison model. The measured relative permittivity shows good correlation with the data from the Ellison model in higher frequencies. For the frequencies below 1 GHz, the deviation is increasing. This can be caused by the used calibration material for the short (copper), which is according to the probe manual intended for the frequencies above 500 MHz [8].

In Fig. 3 the mean deviation δ of the measured temperature dependence of distilled water and model of Ellison is shown. The mean deviation is calculated according to the following equations:

$$\delta\varepsilon'(f, T) = \overline{\varepsilon'}_{measured}(f, T) - \varepsilon'_{Ellison}(f, T) \qquad (4)$$

$$\delta\sigma(f, T) = \bar{\sigma}_{measured}(f, T) - \sigma_{Ellison}(f, T) \qquad (5)$$

where $\overline{\varepsilon'}_{measured}$ is the measured mean value of the relative permittivity and $\bar{\sigma}_{measured}$ is the measured mean value of conductivity. The differences of the relative permittivity without temperature calibration (Fig. 3(a) – dashed lines) are increasing with the frequency and temperature. The deviation is approximately 2.5 units at the upper frequency. In the case of used temperature-dependent calibration, the deviation has decreased and is relatively similar for all measured temperatures. The deviation is ∼0.7 units. Figure 3(b) is representing the deviations of the effective conductivity of our measurements and Ellison model. The solid lines show results with the temperature-dependent calibration and the dashed lines without temperature calibration. For the lower frequencies (below 500 MHz) the deviation is negligible for both cases. With the increasing frequency, the deviation is growing mainly for the measurement without temperature-dependent calibration.

The deviation of the measurement, where the temperature-dependent calibration was used, is fluctuating around zero. The
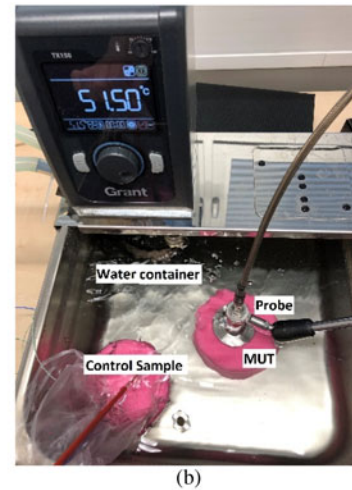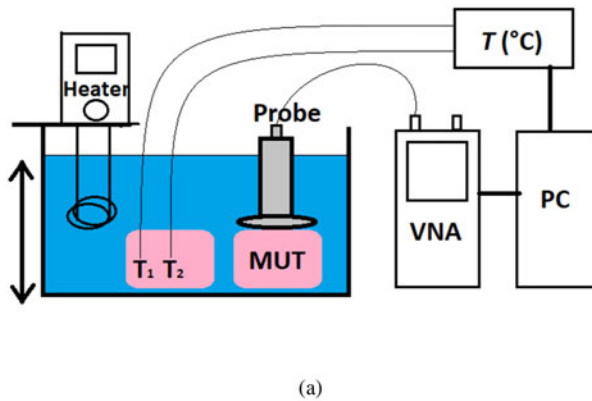
Fig. 1. Measurement setup for the measurement of temperature dependence of tissue mimicking phantoms (a) and the photo of the water container with the coaxial probe and MUT (b).
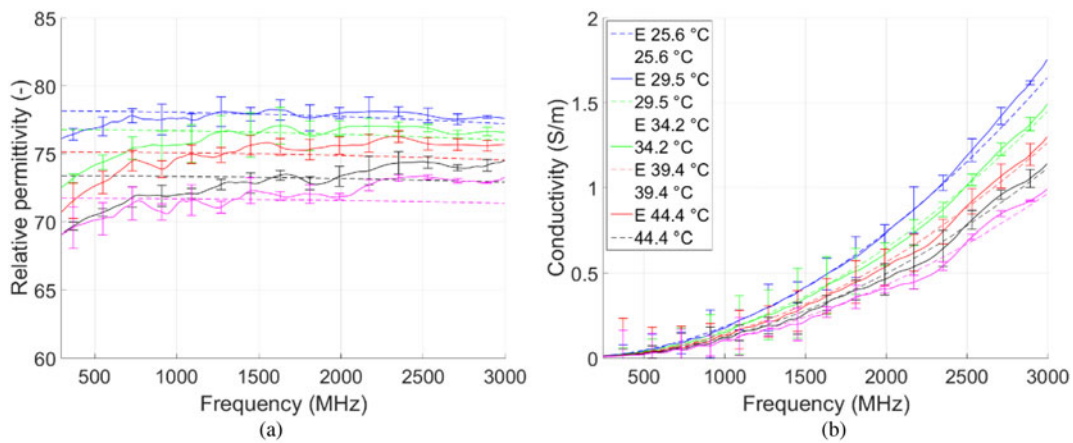
Fig. 2. Measured temperature-dependent relative permittivity (a)* and effective conductivity (b) with combined standard uncertainty u_C (equation (1)) of distilled water (solid lines) in the frequency range of 150–3000 MHz after temperature-dependent calibration compared to the model from Ellison marked as E – (dashed lines).
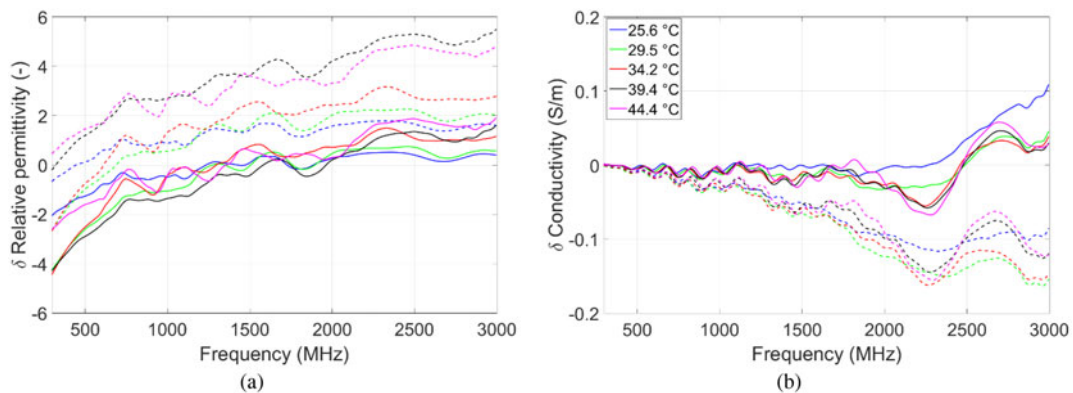
Fig. 3. Differences between the Ellison model and measured temperature-dependent relative permittivity (a) and effective conductivity (b) depending on the calibration procedure. Dashed lines corresponding with the measurement without temperature dependent calibration and solid lines with temperature calibration.

deviation for this measurement is ~0.05 (S/m). It is obvious that the temperature dependent calibration reduced the deviation of the measurement. It is very convenient to perform the temperature-dependent calibration before the measurement.

According to our opinion, the measurement equipment and the proposed measuring procedure ensure the sufficiently precise measurement of the temperature-dependent dielectric parameters of liquids and solids.

Table 1. The composition of proposed muscle phantom, substances in percentages by weight.

Ingredients (%)	Ratio
Distilled water	83.88
PE powder	10.02
TX-151	3.25
Agar powder	2.30
Sodium chloride	0.55

Phantom for microwave imaging

In this section, the proposed measurement method is applied to the new phantom intended for of the microwave imaging systems testing. In our previous study [10], we introduced a new muscle tissue-mimicking phantom. Its dielectric properties were tuned in the way to imitate the frequency dependence of relative permittivity and effective conductivity estimated by Gabriel *et al.* [11]. However, temperature measurements performed on various kinds of biological tissue by Ley *et al.* showed certain differences in behavior [7]. The original phantom was adjusted in order to obtain similar dielectric properties as the current study by Ley *et al.* The composition changes were mainly in the mixture of distilled water, polyethylene (PE) powder, and polysaccharide TX-151. The composition of the final phantom is shown in Table 1, together with other tested versions.

Relative permittivity is mainly dependent on the mixture of distilled water and PE powder, conductivity is highly dependent on the proportion of sodium chloride. As described in [10], for appropriate sample preparation longer time of PE powder mixing is recommended. Plastic wrap is convenient for preventing water evaporation. The vacuum system reduces the number of air bubbles. The appropriate cover is necessary during storage. Therefore, special care should be taken in handling and mixing the substances.

For future studies, it is also very convenient to satisfy temperature dependence requirements, for this purpose measurement in the temperature range of 25–50°C was performed. The final version of phantom also had to meet the required mechanical properties, especially for higher temperature.

Temperature dependent dielectric properties of phantom for microwave hyperthermia and imaging

The measured phantom was of cylindrical shape with sufficient dimensions (70 mm in height with a diameter of 120 mm) to ensure that there is no influence on the surrounding area. The probe was attached directly to the phantom (in the central part) during the whole measurement. Figure 4 shows measured relative permittivity (A) and effective conductivity (B) of the proposed phantom in the temperature region of 25–50°C. The relative permittivity is decreasing with the temperature and frequency nearly linearly in the whole temperature range.

The effective conductivity (Fig. 4(b)) is rising with the temperature to 2300 MHz. Around this frequency, the intersection of the courses can be visible. For the higher frequencies (above 2300 MHz) the effective conductivity is decreasing with the increasing temperature. The measured temperature-dependent dielectric properties of the proposed muscle tissue phantom are fitted to the temperature-dependent Cole–Cole model.

Fitting procedure

A frequency and temperature-dependent Cole–Cole model was determined by measured data. The model enables to simplify the results of measurements and calculate complex relative permittivity and effective conductivity at any frequency and temperature within the given range. The same principle was used to describe the biological tissues data, for example, in [11].

The Cole-Cole model is fitted to the measured data to represent the interaction of the material with the electromagnetic field. The Debye form of the model was used for the materials with constant relaxation times. To model the dispersion accurately, the two pole Cole–Cole model was chosen and fitted. Dispersion behavior is actually present in a broader frequency range, more than it was expected, especially for liquid and solid dielectrics. For this reason, empirical index α was introduced in the original formula. Following two-pole Cole–Cole model is used in this study:

$$\varepsilon^*(f, T) = \varepsilon_\infty(T) + \frac{\Delta\varepsilon_1(T)}{1 + (i\omega\tau_1(T))^{1-\alpha_1}}$$
$$+ \frac{\Delta\varepsilon_2(T)}{1 + (i\omega\tau_2(T))^{1-\alpha_2}} + \frac{\sigma_s(T)}{i\omega\varepsilon_0} \quad (6)$$

where $\Delta\varepsilon_1$, $\Delta\varepsilon_2$ are the dispersion magnitudes, ε_∞ represents the permittivity at very high frequencies (ideally infinite frequency), τ_1, τ_2 are the relaxation times (typically in ns or ps), σ_s is the static conductivity, and $\omega = 2\pi f$ is the angular frequency.

At first Levenberg–Marquardt algorithm was used to fit the two-pole Cole–Cole model to the measured data for each temperature.
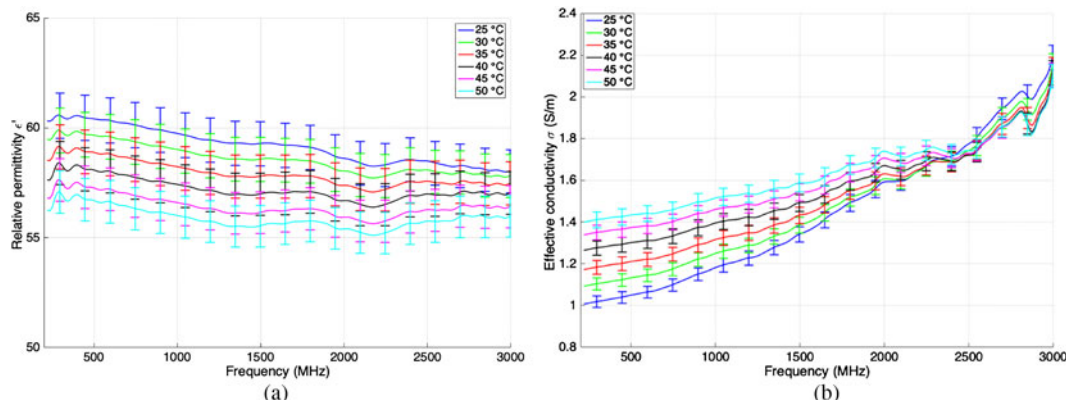
Fig. 4. Measured temperature dependency of the new muscle tissue phantom in the temperature range of 25–50°C.

Table 2. Temperature coefficients of the two-pole Cole–Cole model of the muscle tissue phantom

	n	A_n	B_n	C_n
$\varepsilon_{\infty,fit}$	1	$0.6600 \times 10^{-3}/K^2$	$-0.1303/K$	8.2064
$\Delta\varepsilon_{1,\ fit}$	2	$0.6464 \times 10^{-3}/K^2$	$-0.1293/K$	58.1866
$\tau_{1,\ fit}$	3	$5.4272\ fs/K^2$	$-0.5376\ ps/K$	17.83 ps
$\Delta\varepsilon_{2,\ fit}$	4	$-0.1804 \times 10^{-3}/K^2$	$0.0221/K$	58.6487
$\tau_{2,\ fit}$	5	$-0.1541\ ns/K^2$	$6.3925\ ns/K$	438.3873 ns
$\sigma_{s,\ fit}$	6	$-0.1030 \times 10^{-3}\ mS/K^2$	$0.0234\ mS/K$	465.4264 mS

As there are many fitting parameters, indexes α_1, α_2 were fixed to the value 0.1 for simplification of calculations. The initial values were set according to Gabriel's parameters for muscle tissue. The fitting procedure is taken from [7]. The solution was divided into the real and imaginary part of complex relative permittivity. To obtain the real part, we calculated parameters $\varepsilon_{\infty,\ fit}$, $\Delta\varepsilon_{1,\ fit}$, $\Delta\varepsilon_{2,\ fit}$, $\tau_{1,\ fit}$, $\tau_{2,\ fit}$ by minimizing the mean absolute error over the frequency range of 10 to 3 GHz. After this procedure, the static conductivity sigma was computed to fit imaginary part by the same method as the real part. To get the temperature dependence, a second-order polynomial function with coefficients A_n, B_n, C_n, was used to fit the temperature dependence of the Cole–Cole parameters.

$$\varepsilon_{\infty,fit}(T) = A_1 T^2 + B_1 T + C_1$$
$$\Delta\varepsilon_{1,\ fit}(T) = A_2 T^2 + B_2 T + C_2$$
$$\tau_{1,\ fit}(T) = A_3 T^2 + B_3 T + C_3$$
$$\Delta\varepsilon_{2,\ fit}(T) = A_4 T^2 + B_4 T + C_4 \quad (7)$$
$$\tau_{2,\ fit}(T) = A_5 T^2 + B_5 T + C_5$$
$$\sigma_{s,\ fit}(T) = A_6 T^2 + B_6 T + C_6$$

The final temperature-dependent dielectric properties of the proposed phantom can be computed by the following formula:

$$\varepsilon^*_{fit}(f, T) = \varepsilon_{\infty,fit}(T) + \frac{\Delta\varepsilon_{1,fit}(T)}{1 + (i\omega\tau_{1,fit}(T))^{1-\alpha_1}} \\ + \frac{\Delta\varepsilon_{2,fit}(T)}{1 + (i\omega\tau_{2,fit}(T))^{1-\alpha_2}} + \frac{\sigma_{s,fit}(T)}{i\omega\varepsilon_0} \quad (8)$$
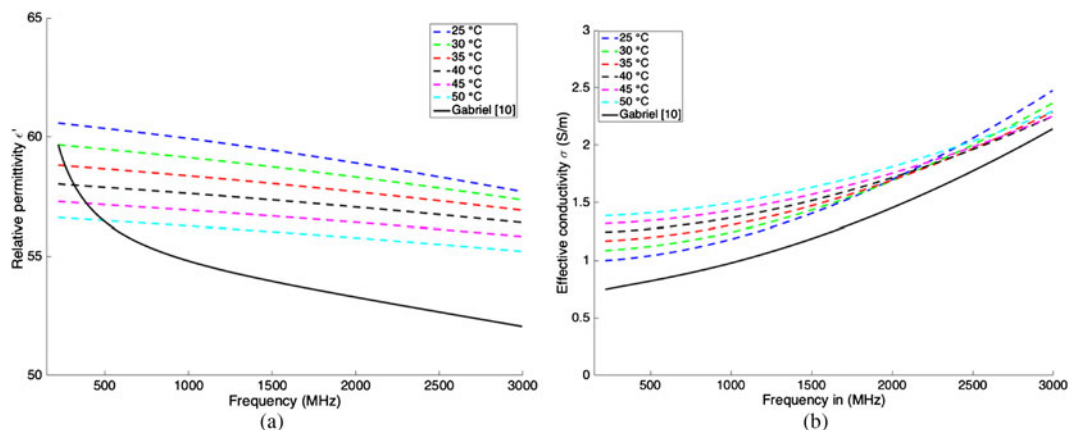
The difference between the measured value and fitted value of the real part of complex relative permittivity and effective conductivity at a certain frequency and temperature indicates the quality of the fitting procedure.

$$\delta\varepsilon'_{measured,fit}(f, T) = \varepsilon'_{measured}(f, T) - \varepsilon'_{fit}(f, T) \quad (9)$$

Effective conductivity was firstly calculated by

$$\sigma_{fit}(f, T) = \omega\,\varepsilon_0\,\varepsilon''_{fit}(f, T) \quad (10)$$

Then the difference is

$$\delta\sigma_{measured,fit}(f, T) = \sigma_{measured}(f, T) - \sigma_{fit}(f, T) \quad (11)$$

Fitting parameters and temperature coefficients of the measured phantom are shown in following Table 2 along with Fig. 5, where the results of the fitted Cole–Cole model are presented.

Figure 5 shows the temperature dependence of the dielectric properties of the muscle tissue phantom based on the fitted parameters of the Cole–Cole model. The graphs from Fig. 5 are based on the temperature-dependent Cole–Cole model – equation (8). The modeled effective conductivity has an intersection at frequency ~2500 MHz. This is corresponding with the results from the measurement. The trend of the temperature dependence is consistent with the models presented by Ley [7] or Gabriel [11].

The efficiency of the fitting procedure is shown in Fig. 6. It representing the differences between measured and modeled data of the muscle tissue phantom. The differences between measured and modeled relative permittivity are lower than 0.7 in case of relative permittivity (A) and lower than 0.4 (S/m) in case of effective conductivity (B).

Conclusion

In this paper, the technique of the measurement of the temperature-dependent dielectric parameters of liquids and solids is presented. This measurement of a quite high accuracy was made for the temperature range between 25 and 50°C. The accuracy was verified by the measurement of the temperature dependency of dielectric parameters of the distilled water and compared
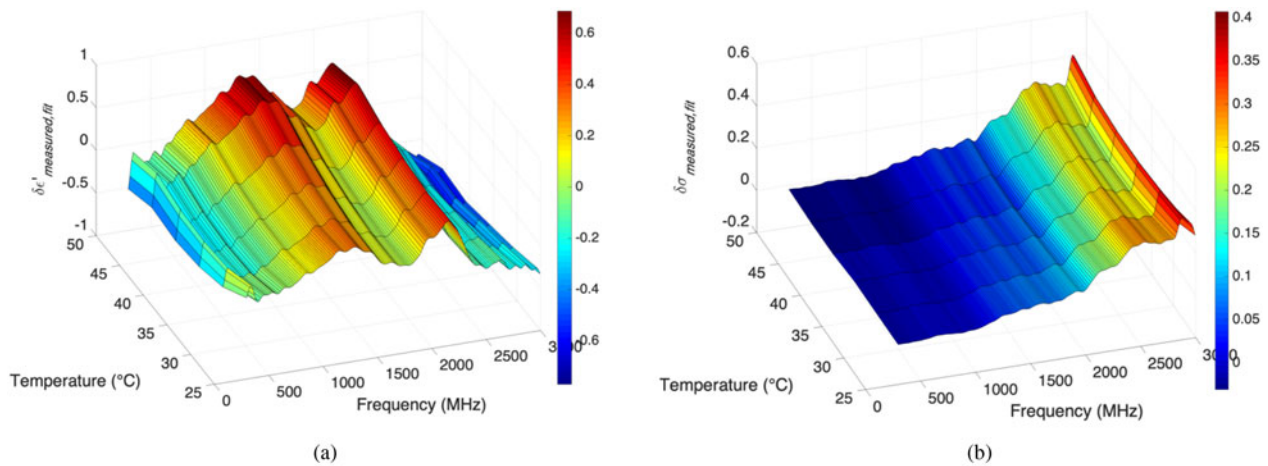
Fig. 5. (a) Relative permittivity and (b) effective conductivity of tissue-mimicking phantom modeled from the fitted two-pole Cole–Cole model.

Fig. 6. Differences between measured and modeled data by the two-pole Cole–Cole model of (a) relative permittivity and (b) effective conductivity.

with literature data. The temperature-dependent calibration of the measurement setup suppresses the difference from the literature model approximately by about 1.8 units for relative permittivity and 0.08 (S/m) for the effective conductivity.

After the verification process, the spectroscopy of a new phantom [10] intended for microwave hyperthermia and temperature imaging via UWB radar was performed. Furthermore, the measured temperature dependencies of dielectric parameters were fitted to the two-pole Cole–Cole model. The differences between measured and modeled data are at an acceptable level. Owing to the measured data and their evaluation, the proposed phantom is suitable for the testing.

6. **Ley S, Fiser O, Merunka I, Vrba J, Sachs J and Helbig M** (2018) Preliminary investigations for reliable temperature dependent UWB dielectric spectroscopy of tissues and tissue mimicking phantom materials. *Proceedings of European Conference on Antennas and Propagation (EuCAP)*, pp. 1–5.

7. **Ley S, Schilling S, Fiser O, Vrba J, Sachs J and Helbig M** (2019) Ultra-wideband temperature dependent dielectric spectroscopy of porcine tissue and blood in the microwave frequency range. *Sensors* **19**, 1707.

8. **DAK 4 MHz to 3 GHz, SPEAG.** Available at https://www.speag.com/products/dak/dak-dielectric-probe-systems/dak-4-mhz-3-ghz/.

9. **Ellison WJ** (2007) Permittivity of pure water, at standard atmospheric pressure, over the frequency range 0–25 THz and the temperature range 0–100°C. *Journal of Physical and Chemical Reference Data* **36**, 1–18.

10. **Kantova M, Fiser O, Merunka I, Vrba J and Tesarik J** (2019) *High-Water Content Phantom for Microwave Imaging and Microwave Hyperthermia*. Singapore: Springer, pp. 779–783.

11. **Gabriel C, Gabriel S and Corthout E** (1996) The dielectric properties of biological tissues: I. Literature survey. *Physics in Medicine and Biology* **41**, 2231–2234.

References

1. **Vrba J** (1993) Evanescent mode applicators for subcutaneous hyperthermia. *Biomedical Engineering, IEEE Transactions on* **40**, 397–407.

2. **Valdagni R and Amichetti M** (1994) Report of long-term follow-up in a randomized trial comparing radiation therapy and radiation therapy plus hyperthermia to metastatic lymphnodes in stage IV head and neck patients. *International Journal of Radiation Oncology*Biology*Physics* **28**, 163–169.

3. **Fiser O, Helbig M, Ley S, Merunka I and Vrba J** (2018) Microwave non-invasive temperature monitoring using UWB radar for cancer treatment by hyperthermia. *Progress In Electromagnetics Research* **162**, 1–14.

4. **Ley S, Fiser O, Merunka I, Vrba J, Sachs J and Helbig M** (2018) Preliminary investigations for non-invasive temperature change detection in thermotherapy by means of UWB microwave radar. *Proceedings of Annual International Conference of the IEEE Engineering in Medicine and Biology Society (EMBC)*, vol. 2018, pp. 5386–5389.

5. **Lazebnik M, Converse MC, Booske JH and Hagness SC** (2006) Ultrawideband temperature-dependent dielectric properties of animal liver tissue in the microwave frequency range. *Physics in Medicine and Biology* **51**, 1941–1955.

Ondrej Fiser received the Ing. (M.Sc.) and Ph.D. degrees in Electrical Engineering (Biomedical Engineering and Radioelectronics) from the Czech Technical University in Prague 2013 and 2018. Currently, he is working as a research assistant and lecturer at the Faculty of Biomedical Engineering, Czech Technical University in Prague. His main interest includes microwave imaging, microwave hyperthermia, and non-invasive temperature measurement.

Sebastian Ley received the Dipl.-Ing. in Media Technology from the Technische Universität Ilmenau (Germany) in 2010. Currently, he is working as a research assistant at the Institute for Biomedical Engineering and Informatics. His research interests include biomedical signal processing and microwave sensing for medical applications, especially for breast cancer detection and non-invasive tissue temperature estimation.

Marko Helbig received the Dipl.-Ing. and Dr.-Ing. degrees in Electrical Engineering (Biomedical Engineering and Signal Processing) from Technische Universität Ilmenau in 1996 and 2007. Currently, he is working as a senior researcher and lecturer at the Institute for Biomedical Engineering and Informatics, Technische Universität Ilmenau. His research interests include biomedical signal processing and ultra-wideband microwave sensing, especially for medical imaging, non-invasive tissue temperature estimation, and remote vital data acquisition.

Jüergen Sachs was Senior Lecturer at Ilmenau University of Technology, Germany. He teaches "Basics of Electrical Measurement Technology", "Measurements in Communications," and "Ultra-Wideband Radar Sensing". Currently, he is with Ilmsens GmbH and deals with the development of ultra-wideband radar and impedance spectroscopy. He is head of several research projects, and inter alia coordinator of European projects for humanitarian demining and disaster relief. His research areas cover RF-signal analysis and RF-system identification; Surface Penetrating Radar for non-destructive testing and medical engineering, ultra wideband methods and their application in high resolution radar and impedance spectroscopy, digital processing of ultra wideband signals, array processing; and design and implementation of new RF device approaches.

Michaela Kantova is master's degree student of Electrical Engineering (Electronics and Communications) at the Czech Technical University in Prague. She is expected to graduate in February 2020. She is focusing on tissue-mimicking materials intended for MW biomedical systems as a student researcher. She studied interstitial hyperthermia applicators in her bachelor thesis.

Jan Vrba received the M.Sc. and Ph.D. degrees from the CTU in Prague (1972 resp. 1976) and since 1993 he is a Full Professor of Radioelectronics at the Dept. of Electromagnetic Field, CTU in Prague. In the period 1972 till 1981 his research was oriented on parametric amplifiers and microstrip resonators. Since 1981 his research activities are focused on medical and industrial applications of microwave technology. He was a member of the team which developed the first system for microwave hyperthermia in cancer treatment in the former Czechoslovakia. He is a member of IEEE, ESHO (European Society for Hyperthermic Oncology), and Electromagnetic Academy. He was awarded by ESHO-Pyrexar Award in 2015.